

Informed Equation Learning

Matthias Werner^{*†‡§} Andrej Junginger^{*} Philipp Hennig[‡]
 Georg Martius[†]

January 8, 2022

Abstract

Distilling data into compact and interpretable analytic equations is one of the goals of science. Instead, contemporary supervised machine learning methods mostly produce unstructured and dense maps from input to output. Particularly in deep learning, this property is owed to the generic nature of simple standard link functions. To learn equations rather than maps, standard non-linearities can be replaced with structured building blocks of atomic functions. However, without strong priors on sparsity and structure, representational complexity and numerical conditioning limit this direct approach. To scale to realistic settings in science and engineering, we propose an informed equation learning system. It provides a way to incorporate expert knowledge about what are permitted or prohibited equation components, as well as a domain-dependent structured sparsity prior. Our system then utilizes a robust method to learn equations with atomic functions exhibiting singularities, as e.g. logarithm and division. We demonstrate several artificial and real-world experiments from the engineering domain, in which our system learns interpretable models of high predictive power.

1 Introduction

Mathematical models formed of equations are key elements in natural sciences to describe phenomena and their underlying principles. Physics, in particular, uses equations to build a coherent description of natural laws. For example, Newton’s and Kepler’s laws or Schrödinger’s equation describe and encode the phenomena of motion, celestial dynamics [Feynman et al., 1965], or quantum mechanics [Ballentine, 1970], respectively. In the engineering domain, mathematical equations are used, e.g., in model-predictive control García et al. [1989] or as components describing complex system. The designed equations then correspond to a hypothesis for the inner system’s behavior and represent its relations and properties. Implementing such control strategies into embedded control units for industrial-scale applications raises various additional constraints like low computational effort, minimal memory usage, low effort of calibration, and generalization to similar systems.

Learning mathematical models in an automated fashion is referred to as *equation learning* or *symbolic regression*. The desired mathematical expressions are usually compositions of *atomic units* consisting of a set of functions $\{f_i\}_{i \leq F}$ and a set of operations that connect the single functions. The former can be, e.g., functions like $\{\sin, \text{sqrt}, \log, \dots\}$ and they can be connected by operations such as $\{+, -, *, /, \circ, \dots\}$.

^{*}corresponding author: matthias.werner@tuebingen.mpg.de

[†]Machine Learning Group at ETAS GmbH, Bosch Group

[‡]Max Planck Institute for Intelligent Systems, Tübingen, Germany

[§]University of Tübingen

Out of these atomic units, equation learning finally tries to infer an analytic expression to describe the relations between the quantities of interest. In this work, we consider a Gaussian regression setting with a parameterized analytical function ψ_θ , to map a D -dimensional input \mathbf{x} to a D' -dimensional output \mathbf{y}

$$\mathbf{y}_i = \psi_\theta(\mathbf{x}_i) + \epsilon, \quad \epsilon \sim \mathcal{N}(0, \gamma^2). \quad (1)$$

Here, θ denotes the parameters, the dataset $(\mathbf{X}, \mathbf{Y}) \in \mathcal{D}$ is assumed to be sampled iid., and it contains N data points each of which has Gaussian noise ϵ with variance γ^2 . The structure of ψ_θ as well as its parameters shall then be inferred from the data. Many contemporary supervised machine learning algorithms optimize for prediction performance alone. Thus, they typically produce unstructured and dense equations, which do not reveal insight into the underlying principles of the data-generating system. Following the principle of Occam’s razor [MacKay, 1992], an equation learning system must trade-off complexity against expressivity to overcome this issue. This typically results in a regularization of the objective function. A generic symbolic regression method using machine learning, named EQL [Martius and Lampert, 2016], replaces standard link functions in a multi-layer feed-forward neural network with atomic units (sin, cos, identity, *) and a Lasso regularization [Tibshirani, 1996]. In principle, this approach can be extended to all continuously differentiable functions with unbounded domains. However, for common atomic units, like division or logarithm with a half-bounded domain \mathbb{D} or with a singularity, continuous optimization of an equation-learning neural network can break down for two reasons: First, the cascading transformation of intermediate results in a deep architecture can project values outside of the constrained input domains. Applying domain-limiting mapping functions, such as softplus, is not ideal since it compromises the final symbolic equation. Second, singularities in the atomic functions or their derivative can lead to large gradients and make optimization highly unstable. A first approach incorporating divisions in the final layer in EQL has been presented in Sahoo et al. [2018]. Their algorithm uses a hard-coded curriculum, which depends on the number of epochs itself. This makes it hard to apply to datasets with different sample sizes. In contrast, our algorithm overcomes those issues and introduces a learnable parameter instead. It is a robust and simple algorithm for atomic units with singularities. We show that this unlocks new classes of functions, as e.g. division, logarithm, etc. in all layers of the iEQL, which is not covered by previous publications.

In general, a large expressivity of the equation learner is desired. The EQL architecture is, in principle, well suited for scaling to large problems. However, the set of possible solutions also grows drastically. Thus, in general, one cannot expect to obtain a symbolic expression that is easily interpretable or that captures the true correspondences. Therefore, we propose to incorporate expert knowledge into the system such that suitable solutions are preferred. Our approach is based on excluding certain combinations of functions or on providing a user-dependent weighting scheme. It was developed in close cooperation with applied engineers. Technically, this is achieved by designing a generalized sparsity regularization, that allows one to choose specific complexities for each atomic unit, and that can flexibly prohibit certain, user-defined function compositions.

In this paper we advance the state-of-the-art in symbolic regression by

- (a) proposing an informed equation learner (iEQL) allowing to incorporating expert knowledge,
- (b) a robust training method for atomic units with singularities (e.g. logarithm and division), and
- (c) showing that interpretable expressions can be discovered from real-world datasets from the engineering domain.

The paper is structured as follows: First, we discuss related work in section 2. In section 3, we introduce the architecture of the iEQL, outline the instance selection criteria and a domain specific complexity measure with its sparsity inducing regularization. Moreover, we present the robust training method for atomic units with singularities. In section 4, we present applications of our method to artificial datasets as well as two real-world applications in the engineering domain, and we conclude in section 5.

2 Related Work

Equation learning studies the relation between input and output data. As a thread within the wider area of explainability, it is of increasing importance to machine learning, which mostly produces black box models. A major challenge in equation learning is to efficiently search the space of possible expressions, which increases exponentially with the number of atomic units required to describe the data relation. Current machine learning methods for equation learning can be separated in bottom up and top down search strategies.

Bottom up methods improve and learn based on individually sampled mathematical expressions until the final expression is simple and accurate. For this purpose, machine learning offers efficient search strategies [Zaremba et al., 2014, Kusner et al., 2017, Li et al., 2019, Lample and Charton, 2020]. A physics-inspired method for equation learning that uses neural networks to identify symmetries and separability within the data was introduced by Udrescu and Tegmark [2020]. Common methods to overcome the exponential growth of the search space are genetic programming and evolutionary algorithms [Langdon et al., 2008, Searson et al., 2010, McRee, 2010]. Algorithms in this vein have been used to automate the discovery of natural laws [Dubčáková, 2011, Schmidt and Lipson, 2009]. However, none of these methods use gradient information about the learned expressions during training. This was addressed in a reinforcement learning formulation by Petersen [2019]. They transformed the discrete optimization to a continuous gradient based optimization scheme via risk-seeking policy gradients, which is a modification of the REINFORCE [Williams, 1992] policy gradient.

Top down search strategies are in contrast to these bottom up search strategies. They start with a highly general expression and try to omit irrelevant parts during training until a simple but accurate expression is found. This idea is also applied by the EQL [Martius and Lampert, 2016], which defines a neural network architecture as general expression. It represents all possible symbolic expressions within its architecture. During training irrelevant parts get pruned until the EQL itself represents a simple but accurate equation. A similar architecture has been studied by Long et al. [2019] on differential equations, and the integration of an EQL-like architecture within other deep learning frameworks has been studied by Kim et al. [2020]. Also in physics it has been used to obtain analytical expressions of classical free energy functionals in Lin et al. [2020]. Generally, these top down methods have the advantage that they permit the use of efficient continuous gradient based optimization. In contrast to [Martius and Lampert, 2016, Sahoo et al., 2018], which used L_1 regularization, we use L_0 regularization [Louizos et al., 2018], which does not shrink the weights during training and allows to naturally align a domain specific complexity measure with the regularization. A first approach to use divisions in EQL has been presented by Sahoo et al. [2018]. Their architecture only considers division units in the final layer. We propose a robust training method for atomic units with singularities in general that does not require a predefined curriculum and allows to using division units in all layers.

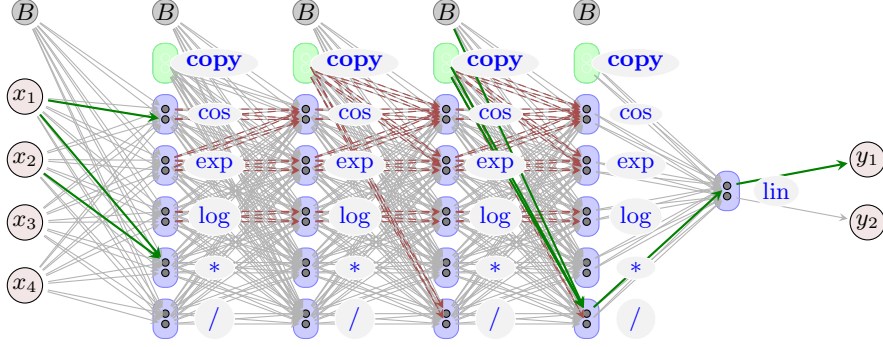


Figure 1: Exemplary setup of the iEQL with 4 hidden layers, three types of unary atomic units $\{\cos, \exp, \log\}$ and two types of binary atomic units $\{*, /\}$ per layer. The copy units contains all units from all previous layers. The red dashed arrows mark forbidden connections (see equation 4) which are removed, also from the copy units. After successful training, the iEQL represents the desired equation. The green connections visualize an exemplary model for the equation $y_2 = 0$ and $y_1 = (x_2 \cdot x_1) / (\cos x_1 + 1.5)$.

3 Method

3.1 Architecture of the iEQL

Our goal is to identify a compact equation describing data accurately. A standard neural network as a universal function approximator is representing a large uninterpretable equation. Replacing units of a neural network with various building blocks of equations and forcing a sparse connection in the network can yield simple and interpretable mathematical equations. The proposed architecture, see Figure 1, of a multi-layered feed-forward equation learning network is similar to previous work by Martius and Lampert [2016], Sahoo et al. [2018]. It consists of L layers, whose $L - 1$ hidden layers correspond to the maximum number of function compositions. Each hidden layer applies a non-linear transformation, which consists of u unary atomic units $f_{i \leq u} : \mathbb{R} \rightarrow \mathbb{R}$ and v binary atomic units $g_{j \leq v} : \mathbb{R} \times \mathbb{R} \rightarrow \mathbb{R}$. The latter can be, e.g., division a/b or multiplication $a \cdot b$. We apply an affine transformation on the output of all preceding layers, including the input data ($\mathbf{y}^0 := \mathbf{x}$), instead of just the previous one (similarly used in dense-nets [Huang et al., 2016])

$$\mathbf{z}^l = \mathbf{W}^l \hat{\mathbf{y}}^{l-1} + \mathbf{b}^l, \text{ with: } \hat{\mathbf{y}}^{l-1} = (\mathbf{y}^0, \dots, \mathbf{y}^{l-1}) \quad (2)$$

$$\mathbf{y}^l = (f_1(z_1^l), \dots, f_u(z_u^l), g_1(z_{u+1}, z_{u+2}), \dots). \quad (3)$$

Those skip connections allow identified sub-solutions (terms in the equation) to be available with no additional cost to all subsequent layers. Figure 1 visualizes a possible layout of the architecture, in which all previous' layers output is marked by the **copy** units. Naturally, the skip connections favor less nested expressions and allow to ignoring unnecessary layers. Moreover, the search for appropriate hyperparameters is simplified as the initial network can be chosen larger and more complex. Depending on the application, certain combinations of atomic units like

$$\cos(\cos(\cdot)) \quad \cos(\exp(\cdot)) \quad \exp(\exp(\cdot)) \quad \log(\log(\cdot)) \quad (4)$$

with respective arguments can be undesirable (i.e. they should only be chosen rarely), or they might not make sense at all. *Expert* and *domain knowledge* can provide such information on possible equation structures. Therefore, all forbidden connections are removed from the architecture as shown in figure 1. That way, an expert finally

Table 1: Domain specific complexity factors c_u for different atomic units. No preference is denoted as *plain*. For the real world applications (power loss of an electric machine (section 4.3) and torque model of a combustion engine (section 4.4)). We use values suggested by domain experts denoted as *motor*.

	$+/-$	$*$	$/$	x^2	\log	$\sqrt{}$	\exp	\cos
plain	1	1	1	1	1	1	1	1
motor	1	2	5	2	5	3	5	10

decides which combinations to use and which to exclude. Such information could not be used in previous work by Martius and Lampert [2016], Sahoo et al. [2018], since the respective architecture relied on linear units, which accumulate output of all previous layer in an affine transformation. That made it impossible to remove certain combinations. However, with the present framework based on copy units, it is easily possible to prohibit certain combinations of atomic units in the iEQL.

3.2 Model Selection Criteria

We apply model selection criteria V^{int} , $V^{\text{int-S}}$ and $V^{\text{int\&ex}}$ proposed by Sahoo et al. [2018] to select a good equation amongst all found equations. They are based on a normalized validation error $\tilde{\nu}_{\text{in}}$, normalized complexity \tilde{s}^2 and a normalized extrapolation validation error $\tilde{\nu}_{\text{ex}}$, which requires some points (here 40) from the extrapolation domain

$$V^{\text{int}} = \arg \min[\tilde{\nu}_{\text{int}}^2] \quad (5)$$

$$V^{\text{int-S}} = \arg \min[\tilde{\nu}_{\text{int}}^2 + \tilde{s}^2] \quad (6)$$

$$V^{\text{int\&ex}} = \arg \min[\tilde{\nu}_{\text{int}}^2 + \tilde{\nu}_{\text{ex}}^2]. \quad (7)$$

3.3 Complexity Measure

The “complexity” of an equation — not the computational complexity per se, but whether an expert would consider it “basic” or “involved”, depends both on the number of terms and a domain specific complexity cost of each atomic operation. To capture this aspect, we use a weighted sum of the number of parameters as a measure of complexity. This is a commonly accepted way to introduce domain knowledge in symbolic regression, e.g. in evolutionary search [Dubčáková, 2011]. An expert defines domain-specific complexity factors c_u for each atomic unit type u . The c_u can depend on soft criteria, like domain or personal experience, but also quite concretely on computational cost. A specific choice of the complexity factors c_u for our experiments is shown in table 1.

3.4 Sparsity Inducing Method

Sparsity inducing regularization is necessary to extract interpretable and compact equations from the iEQL. We are able to directly optimize for the complexity measure, described in section 3.3, as regularization \mathcal{L}_C and the mean squared error as data loss \mathcal{L}_D :

$$\mathcal{L}_D = \frac{1}{N} \sum_{i=1}^N \|\mathbf{y}_i - \text{iEQL}(\mathbf{x}_i, \mathbf{W})\|_2^2, \quad \mathcal{L}_C = \sum_{u=1}^U c_u \|\mathbf{W}_u\|_0. \quad (8)$$

\mathbf{W}_u represents all weights, which correspond to an atomic unit type. Opposed to the L_1 regularization scheme used by Martius and Lampert [2016], Sahoo et al. [2018], we

use a differentiable version of L_0 -regularization [Louizos et al., 2018]. A final retraining of the pruned network is not necessary anymore, as it does not induce shrinkage on the actual values of the weights. Minor modifications are required to apply the original implementation of Louizos et al. [2018] to weights instead of nodes. Each weight is multiplied by a non-negative stochastic Bernoulli distributed gate $g_j \sim \text{Ber}(\pi_j)$. The dropout rate of each weight is thus given by $1 - \pi_j$. The expectation of a weight being relevant is given by π_j . Those gates learn collectively which weights are relevant. The expected objective is then

$$\mathcal{L} = \mathbb{E}_{q(\mathbf{g}|\pi)} \left[\frac{1}{N} \sum_{i=1}^N \|\mathbf{y}_i - \text{iEQL}(\mathbf{x}_i, \mathbf{W})\|_2^2 \right] + \lambda \sum_{u=1}^U c_u \sum_{j=1}^{|W_u|} \pi_j^u. \quad (9)$$

$|W_u|$ is the total number of weights that correspond to an atomic unit type (u). Further details on the variational optimization scheme are given in appendix A.3.

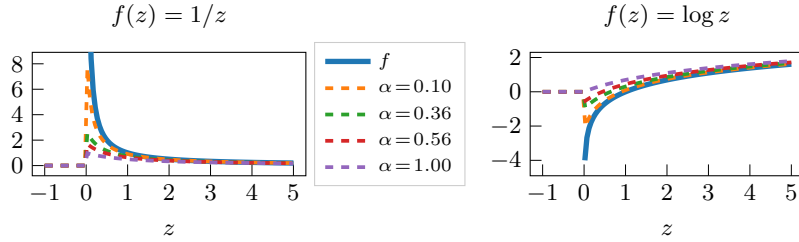


Figure 2: Relaxation of the division (left) and logarithm (right) for different values of α .

3.5 Atomic Units with Singularities

Our algorithm is designed for atomic units with singularities¹ $f : \mathbb{D} \rightarrow \mathbb{R}$ on a half-bounded domain $\mathbb{D} \equiv (a, \infty)$ exhibiting a singularity at a (e.g. $\log : (0, \infty) \rightarrow \mathbb{R}$ with a singularity at $a = 0$). It also applies to division units c/d under the assumption that real systems do not diverge in the domain of application. Then, it is sufficient to only consider the positive branch of the hyperbola $1/d$ and let c choose the sign. Cascading transformation of intermediate results in the deep architecture of the iEQL can project values outside of the constrained input domains of singular units. Therefore, the domain \mathbb{D} of a singular unit is continuously extended to \mathbb{R} to avoid forbidden inputs during training (see equation 11), similar to Sahoo et al. [2018]. During training, an additional penalty \mathcal{L}_{su} is necessary to constrain the solution space of the iEQL to networks that respect the domain \mathbb{D} of all its singular units $f_u(z_u)$

$$\mathcal{L}_{\text{su}} = \frac{1}{N} \sum_{i=1}^N \sum_{u \in \mathcal{SU}} \mathcal{L}_{\text{su}}^u(z_i^u), \quad \mathcal{L}_{\text{su}}^u(z_i^u) = \begin{cases} 0, & \text{for } z_i^u > a, \\ |a - z_i^u|, & \text{for } z_i^u \leq a. \end{cases} \quad (10)$$

The set of all singular units in the iEQL is given by \mathcal{SU} . Still, training can be corrupted by unconstrained values and exploding gradients in the neighborhood of the singularities. Therefore, we propose a learnable relaxation of the singular units that does not compromise the final symbolic equation. It is shown in figure 2 for the logarithm and division. The input z is shifted $\hat{z} = z + \alpha$ by a learnable positive relaxation-parameter $\alpha = \log(1 + e^{\hat{\alpha}}) > 0$

$$\hat{f}(\hat{z}) = \begin{cases} f(z + \alpha), & \text{for } z > a, \\ 0, & \text{for } z \leq a \end{cases}. \quad (11)$$

¹we refer to them as singular units

Since the input $z = Wy + b$ is an affine transformation of the previous layer with bias b the relaxation-parameter α can be safely added to the bias and does not affect the structure of the final equation. This method assures that, during and after training, the maximum absolute value in the neighborhood of the singularity is smaller than $|f(a + \alpha)|$ and the maximum value of the derivative is smaller than $|\partial f(a + \alpha)|$ on the training dataset. The final objective function is thus a sum of data loss \mathcal{L}_D , regularization \mathcal{L}_C and domain penalty \mathcal{L}_{su} with domain penalty strength δ

$$\mathcal{L} = \mathcal{L}_D + \delta \mathcal{L}_{su} + \lambda \mathcal{L}_C. \quad (12)$$

In order to guarantee that the domain constraints on singular units also hold on the extrapolation area and that the order of magnitude does not change drastically on extrapolation data, intrinsic penalty epochs are necessary as proposed in Sahoo et al. [2018]. The bound-penalty \mathcal{L}_{bound} is given by

$$\mathcal{L}_{bound} = \frac{1}{N} \sum_{i=1}^N \arg \max(|\text{iEQL}(\mathbf{x}_i, \mathbf{W})| - B, 0) \quad (13)$$

For an intrinsic penalty epoch, we randomly sample N input data points from the test area without labels. Then the iEQL is trained on the loss function

$$\mathcal{L}_{penalty} = \delta \mathcal{L}_{su} + \delta \mathcal{L}_{bound}. \quad (14)$$

4 Experiments

We demonstrate the application of the iEQL to four different use cases. The first one is to learn complex equations on simulated data of several equations. The second use case is a simulated ambiguity dataset, with which we demonstrate how to incorporate expert knowledge to influence the outcome of the equation learner. Additionally, we study the relative frequency of selected atomic units in found equations with and without expert knowledge on a simulated dataset and a real world dataset. Use cases three and four both address real-world applications in industry determining expressions for the power loss of an electric machine and a torque model of a combustion engine. All experiments are performed using an iEQL with four hidden layers. Each hidden layer has $\{\cos, \exp, \log, \sqrt{}, x^2, *, /\}$ as atomic units, and each atomic unit is applied four times in each layer. Combinations from equation 4 are prohibited. We compare the iEQL to five different algorithms:

- EQL⁺, a state-of-the-art method from Sahoo et al. [2018] with atomic unit types $\{\sin, \cos, *, \text{identity}\}$ in each hidden layer and division in the final layer,
- a multi-layer perceptron (MLP) with tanh activation functions and five hidden layers with 50 neurons each,
- a genetic algorithm (PySR, Cranmer [2020]) with two different configurations GA1 and GA2,
- a Gaussian Process (GP) for the real world datasets, calculated with ASCMO [Hoffmann et al., 2015], which is a standard tool from the engineering domain,
- the mean predictor (MP) on the train set.

Further details on training and parameter settings are outlined in appendix A.1. All experiments are executed five times, and we report median, minimum and maximum (in sub and superscript) of root mean squared error on test datasets.

Table 2: Complex equations on which the iEQL is evaluated. Most functions are gathered from different papers on symbolic regression. A star (*) indicates that input and output were scaled.

Data-set	Ground truth equation	motivated from	Domain	
			train	test
S0	$y = (1 - x_2^2)/(\sin(2\pi x_1) + 1.5)$		$[-1, 1]^4$	$[-2, 2]^4$
S1	$y = [\sin(\pi x_1) + \sin(2\pi x_2 + \pi/8) + x_2 - x_3 x_4]/3$	Sahoo et al. [2018]	$[-1, 1]^4$	$[-2, 2]^4$
S2	$y = [\sin(\pi x_1) + x_2 \cos(2\pi x_1 + \pi/4) + x_3 - x_4^2]/3$	Sahoo et al. [2018]	$[-1, 1]^4$	$[-2, 2]^4$
S3	$y = [(1 + x_2) \sin(\pi x_1) + x_2 x_3 x_4]/3$	Sahoo et al. [2018]	$[-1, 1]^4$	$[-2, 2]^4$
S4*	$y = (3.0375 x_1 x_2 + 5.5 \sin^{9/4}(x_1 - 2/3)(x_2 - 2/3))/5$	Jin et al. [2019]	$[-1, 1]^4$	$[-2, 2]^4$
S5*	$y = \frac{(5x_1)^4}{(5x_1)^4+1} + \frac{(5x_2)^4}{(5x_2)^4+1}$	Trujillo et al. [2016]	$[-1, 1]^4$	$[-2, 2]^4$
S6*	$y = ((1 - x_1)^2 + (1 - x_3)^2 + 100(x_2 - x_1^2)^2 + 100(x_4 - x_3^2)^2)/1500$	4D-Rosenbrock	$[-1, 1]^4$	$[-2, 2]^4$
A1*	$y = (1.5e^{1.5x_1} + 5 \cos(3x_2))/10$	Jin et al. [2019]	$[-1, 1]^4$	$[-2, 2]^4$
A2*	$y = \log(2x_2 + 1) - \log(4x_1^2 + 1)$	Trujillo et al. [2016]	$[0, 1]^2$	$[0, 2]^2$
A3*	$y = \frac{\exp(-(4x_1-0.4)^2)}{1.2+(4x_2-1.9)^2}$	Trujillo et al. [2016]	$[0, 1]^2$	$[0, 2]^2$
A4*	$y = \frac{x_3+1}{3\pi^2} \frac{(5x_1+1)^3}{\exp\left(\frac{(x_3+1)(5x_1+1)}{(x_4+1)(0.5x_2+1)}\right) - 1}$	Udrescu and Tegmark (2020)	$[0, 1]^4$	$[0, 2]^4$

Table 3: Learning complex equations S0-S6: median, minimum and maximum (in sub and superscript) of root mean squared error (RMSE) on test datasets. Baselines are the EQL⁺ from Sahoo et al. [2018], a genetic algorithm (GA) from Cranmer [2020], a multi-layer perceptron (MLP) and the mean predictor (MP) on the train dataset.

	S0	S1	S2	S3	S4	S5	S6
MP	1.57	0.66	0.75	0.64	1.17	0.44	0.82
MLP	1.11 ^{1.17} _{1.04}	0.45 ^{0.54} _{0.35}	0.41 ^{0.42} _{0.39}	0.36 ^{0.37} _{0.34}	0.65 ^{0.70} _{0.57}	0.07 ^{0.15} _{0.02}	0.65 ^{0.66} _{0.65}
GA1	1.07 ^{1.58} _{0.91}	0.77 ^{0.77} _{0.77}	0.33 ^{0.35} _{0.01}	0.01 ^{0.47} _{0.01}	1.20 ^{1.23} _{1.07}	0.29 ^{0.29} _{0.29}	0.82 ^{0.82} _{0.82}
GA2	0.39 ^{1.47} _{0.01}	0.66 ^{0.77} _{0.01}	0.37 ^{0.77} _{0.01}	0.60 ^{1.78} _{0.58}	0.01 ^{0.01} _{0.01}	0.08 ^{0.42} _{0.01}	4.26 ^{inf} _{0.74}
EQL ⁺	0.01 ^{0.12} _{0.01}	0.01 ^{0.17} _{0.01}	0.01 ^{0.05} _{0.01}	0.01 ^{0.01} _{0.01}	0.01 ^{1.38} _{0.01}	0.01 ^{0.01} _{0.01}	0.01 ^{0.02} _{0.01}
iEQL	0.01 ^{0.01} _{0.01}	0.01 ^{0.01} _{0.01}	0.01 ^{0.01} _{0.01}	0.01 ^{0.01} _{0.01}	0.01 ^{0.01} _{0.01}	0.01 ^{0.01} _{0.01}	0.01 ^{0.01} _{0.01}

4.1 Learning Complex Equations

We evaluate the iEQL on two different sets of ground truth equations shown in table 2: (S0–S6) with $\{\pm, \sin, \cos, *, /\}$ as operations and (A1–A4) also including $\{\log, \exp\}$. A two dimensional contour plot of all datasets is shown in appendix figure 6. Most functions are gathered from different papers on symbolic regression. A star (*) indicates that input and output values were scaled. We closely follow the evaluation strategy proposed in Sahoo et al. [2018] with their model selection criteria $V_{int\&ex}$ with 40 extrapolation points (see section 3.2) on the found equations of iEQL, EQL⁺ and GA. Training datasets consist of 10^4 randomly sampled data points in the train domain. Outputs are corrupted with standard normal noise of standard deviation $\gamma = 0.01$. For validation 10% of the training dataset is used. Test datasets consist of 10^3 randomly sampled data points from the test domain (see table 2). Note that for the equations S0–S6 and A1 with their four dimensional input, the extrapolation area of the test dataset is 15 times larger than its interpolation area. The included extrapolation domain is a good indicator for whether or not the ground truth has been found.

Table 4: Learning complex equations (A1–A4): median, minimum and maximum (in sub and superscript) of root mean squared error (RMSE) on test datasets. Baselines are the EQL⁺ from Sahoo et al. [2018], a genetic algorithm (GA) from Cranmer [2020], a multi-layer perceptron (MLP) and the mean predictor (MP) on the train dataset.

	A1	A2	A3	A4
MP	0.88	1.09	0.19	0.66
MLP	0.67 _{0.64} ^{0.70}	0.24 _{0.22} ^{0.25}	0.01 _{0.01} ^{0.02}	0.39 _{0.37} ^{0.40}
GA1	0.82 _{0.28} ^{1.11}	0.35 _{0.26} ^{0.62}	0.14 _{0.14} ^{0.19}	0.60 _{0.56} ^{0.66}
GA2	0.28 _{0.04} ^{0.45}	0.10 _{0.06} ^{0.51}	0.10 _{0.04} ^{0.77}	0.35 _{0.28} ^{0.60}
EQL ⁺	0.09 _{0.09} ^{0.11}	0.09 _{0.06} ^{0.19}	0.02 _{0.01} ^{0.33}	0.36 _{0.22} ^{1.89}
iEQL	0.02 _{0.01} ^{0.06}	0.03 _{0.02} ^{0.05}	0.01 _{0.01} ^{0.02}	0.07 _{0.07} ^{0.13}

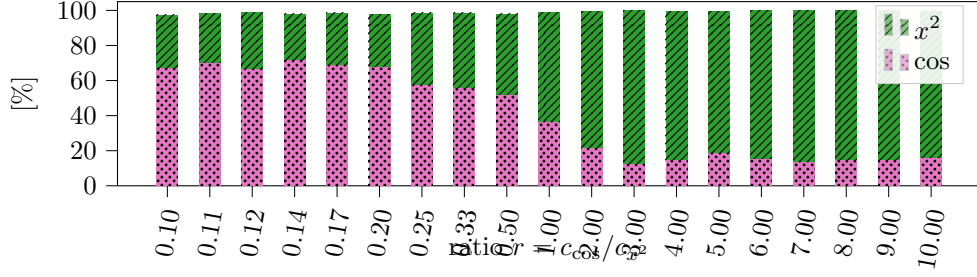
All three network-based models (MLP, EQL⁺, iEQL) can fit the training data perfectly. Their prediction error on training and validation data is at noise level for all datasets S0–S6, and A1–A4. Table 3 shows the results on the test datasets for S0–S6. Unsurprisingly, the MLP is not able to capture the data-generating function (ground truth) by any means. Therefore, it is not able to perform well on the test domain, which includes large extrapolation domains, except for equation A3, which is mainly zero in the extrapolation domain. In contrast, GA, EQL⁺, and iEQL can learn meaningful equations, which can extrapolate on the test domain. If the correct equation has been identified by the $V^{\text{int}\&\text{ex}}$ criteria, the test RMSE is expected to be at noise level. The genetic algorithm (GA1) captures the data generating function on the datasets S2 and S3 at least in one experiment and GA2 on the datasets S0, S1, S2, S4 and S5. On datasets S0–S6 the iEQL captures the data generating function reliably for all five runs as shown in table 3. Despite its larger expressivity, with $\{\cos, \exp, \log, \sqrt{\cdot}, x^2, *, /\}$ atomic units, it even outperforms the EQL⁺ architecture, which uses just the necessary atomic units $\{\cos, \sin, *, /\}$. Equations A1–A4 are more difficult to learn. iEQL outperforms all baselines as shown in table 4.

4.2 Expert Knowledge

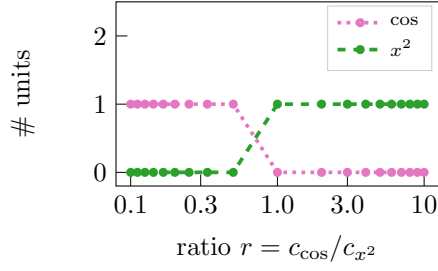
Expert knowledge is especially important if there are several possible equations for an ambiguous dataset. Incorporating this knowledge into the complexity measure as well as the regularization can decide whether the right equation is found. The following experiment studies how different sets of complexity factors affect the relative frequency of atomic units in the set of found equations as well as the importance of complexity factors for the selection criteria $V^{\text{int}}\text{-S}$, which is applied to the set of found equations. The selection criteria $V^{\text{int}\&\text{ex}}$ is not suited for this experiment, since it ignores the model complexity. In order to construct an ambiguous dataset we choose the ground truth

$$y = 8 \cos(0.5x) - 4 \quad (15)$$

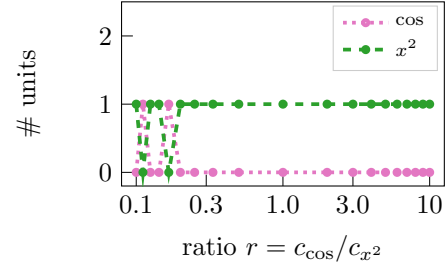
which, close to $x = 0$, can be modeled equivalently by a \cos function or a polynomial of degree 2. The output is corrupted with standard normal noise $\mathcal{N}(0, 0.01^2)$. The training dataset consists of 10^4 randomly sampled data points on the train domain $[-1, 1]$. It resembles a parabola. We study 9 configurations that prefer a periodic structure $c_{\cos} \in \{1/2, 1/3, \dots, 1/10\}$ and 9 configurations that prefer a polynomial structure $c_{x^2} \in \{1/2, 1/3, \dots, 1/10\}$ as well as the plain configuration. For each complexity cost ratio $r = c_{\cos}/c_{x^2}$ we calculate the relative frequency of atomic units for each of the 78 found equations (number of different regularization strength, see appendix A.1).



(a) relative frequency of atomic units



(b) $V^{\text{int}}\text{-S}$ with complexity factors



(c) $V^{\text{int}}\text{-S}$ without complexity factors

Figure 3: The effect of expert knowledge is quantified by means of an ambiguous dataset with its ground truth given by equation 15. For each complexity cost ratio $r = c_{\cos}/c_{x^2}$ the relative frequency of atomic units is calculated for each found equation. Panel (a) shows the average of all those relative frequencies for \cos and x^2 units. The number of \cos and x^2 units appearing in the selected equation depending on the complexity cost ratio is shown in panel (b) selected with $V^{\text{int}}\text{-S}$ with complexity factors and in panel (c) with $V^{\text{int}}\text{-S}$ without complexity factors.

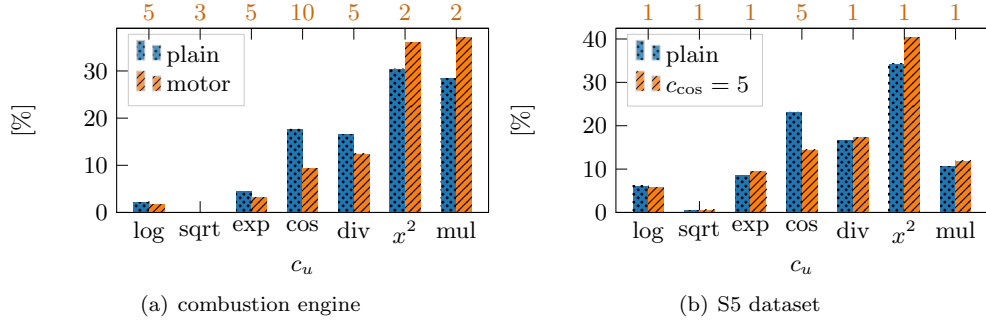


Figure 4: Relative frequency of atomic units with and without domain specific factors over all found equations (5 experiments, each with 78 different regularization strength, see appendix A.1) of the combustion engine experiments in (a) and all found equations of the S5 dataset experiments in (b). Domain specific complexity factors c_u are shown in the upper x-axis.

Figure 3(a) shows the average of all those relative frequencies for \cos and x^2 units. As desired the relative frequencies follow the prior. Ratios with $r < 1$ prefer \cos units and ratios with $r > 1$ prefer x^2 units. Without any further information ($r = 1$) a polynomial solution seems very plausible. It turns out that iEQL does not converge to all kinds of simple ambiguous solutions with the same probability. Often, certain solutions are more likely to converge to. In this experiment, for instance, iEQL predominantly uses x^2 units without a biased preference ($r = 1$). Figure 3(b) shows the number of \cos and x^2 units appearing in the selected equation depending on the complexity cost ratio. Ratios with $r < 1$ prefer a periodic equation and ratios with $r > 1$ prefer a polynomial equation. As desired, the prior is followed in case of such a strong ambiguity. Without complexity factors a polynomial solution is mostly selected as shown in figure 3(c). Hence, complexity factors are crucial to select the correct equation with respect to the prior. Since in this case both types of found equations have the same complexity we found that the ADAM optimizer converges better for x^2 atomic units. This leads to the preference of polynomial solutions.

Figure 4(a) shows the impact of motor specific complexity factors (shown in table 1) on the relative frequencies of atomic units evaluated on all found equations (5 experiments, each with 78 different regularization strength, see appendix A.1) on the real world dataset ‘torque of an internal combustion engine’, which is introduced in section 4.4. The motor specific complexity factors clearly reduce the relative frequency of $\{\exp, \cos, /\}$ atomic units and enhances polynomial structures with $\{x^2, *\}$ units. The $\sqrt{}$ unit has been barely chosen at all. This coincides with the expected behavior. Figure 4(b) shows the impact of penalizing \cos units with ($c_{\cos} = 5$) on a more sophisticated synthetic dataset (S5), as expected the relative frequency of the cosine units is reduced.

4.3 Power Loss of an Electric Machine

In this section, we address with the power loss of an electric machine a relevant problem in the industrial domain [Buchner et al., 2020]. Increasing requirements on control of electric machines in automotive power trains lead to the necessity of more and more sophisticated and complex models to describe the system. Those models have to be able to capture non-linear effects at different components in the system, as in the dataset for the power loss of an electric machine. Further, those models have to be minimal in computational effort and memory demand due to embedded

Table 5: Data properties for the power loss of an electric machine. The train domain covers just 80% the range of operation. Except for rotor temperature T_{rot} which has just three different operation points.

Quantity	Test Domain	Train Domain	Description	Type
I_D [A]	[1, 525]	[76, 451]	direct current	input
I_Q [A]	[1, 525]	[76, 451]	quadratic current	input
T_{rot} [°C]	[-20, 150]	[-20, 150]	rotor temperature	input
n_{mtr} [rpm]	[1, 16000]	[2001, 14001]	motor speed	input
P_{mod} [W]	[0, 4558]	[95, 3364]	power loss	output

Table 6: Results on real-world datasets. Reported are median, minimum and maximum (in sub and superscript) of root mean squared error (RMSE) on the real world test datasets. Domain knowledge is used for iEQL_{motor} as given in table 1. We use the model selection criteria V^{int} -S and state the number of active parameters. For the combustion engine dataset we also present the best validation models selected with V^{int} .

	electric machine [W]		combustion engine [Nm]			
	V^{int} -S	#param.	V^{int} -S	#param.	V^{int}	#param.
MP	1042.70		60.17		60.17	
GP	0.92		1.79		1.79	
GA1	188.40	^{347.93} _{155.84}	9 ⁹ ₃	16.79	^{22.37} _{13.35}	7 ¹¹ ₅
GA2	230.23	^{230.23} _{230.23}	8 ⁸ ₈	22.37	^{22.37} _{16.79}	5 ⁷ ₅
EQL ⁺	0.03	^{0.04} _{0.03}	10 ¹⁴ ₇	1.75	^{1.96} _{1.55}	95 ¹²⁹ ₇₀
iEQL	0.03	^{0.03} _{0.02}	6 ⁶ ₆	2.48	^{3.04} _{2.18}	65 ⁷⁹ ₄₂
iEQL _{motor}	0.02	^{0.02} _{0.02}	6 ⁶ ₆	3.17	^{6.16} _{2.90}	32 ⁴⁸ ₁₅
					1.60	^{1.79} _{1.39}
					339	³⁸⁶ ₁₇₀

hardware and latency constraints in the range of micro-seconds.

In this industrial dataset, the power loss of a winding head is measured depending on the direct current I_D , quadratic current I_Q , rotor temperature T_{rot} , and motor speed n_{mtr} . The data was measured at stationary operation points. It contains 24684 data points measured at equidistant variations of the quantities listed in table 5 within their range of operation. The test dataset contains unseen data from the entire domain and training dataset contains data only from 80% of its range of operation. Further details on data preparation are given in appendix A.2.

We use the model selection criteria V^{int} -S on the found equations of iEQL, EQL⁺ and GA. Results are shown in table 6. iEQL and EQL⁺ outperform the genetic algorithm (GA) and the Gaussian Process (GP) even on the training data and provide very accurate predictions on the test set. The GP does not capture the underlying relationship as can be seen at the large test RMSE. A closer look at the results of the genetic algorithm revealed that the internal selection criteria of GA led to competitive results: GA1 with $0.47 \frac{159.11}{0.02}$ W and $19 \frac{23}{9}$ parameters and GA2 with $0.02 \frac{0.16}{0.02}$ W and $17 \frac{19}{15}$ parameters. iEQL needs even fewer parameters than EQL⁺. This is due to the use of copy units, which allow to reusing features from previous layers directly. We emphasize that, out of the large set of possible functions, the iEQL reliably extracted a simple quadratic equation that suitably describes the dataset. To highlight the simplicity of the iEQL’s result, we state in the following the structure of the selected equation, which is the same for all 5 experiments

$$y = w_1 I_Q + w_2 I_D + w_5 (w_3 I_D + b_1)^2 + w_6 (w_4 I_Q + b_2)^2 + b_3. \quad (16)$$

Table 7: Data properties for the torque model of an internal combustion engine.

Quantity	Unit	Min.	Max.	Description	Type
ϕ_{ex}	°Crank	−20	20	exhaust camshaft	input
ϕ_{in}	°Crank	−4	36	intake camshaft	input
r_l	%	13	86	relative load	input
ϕ_{ign}	°Crank	−27	61	ignition angle	input
n_{eng}	rpm	597	6000	engine speed	input
M_{eng}	Nm	−38	261	engine torque	output

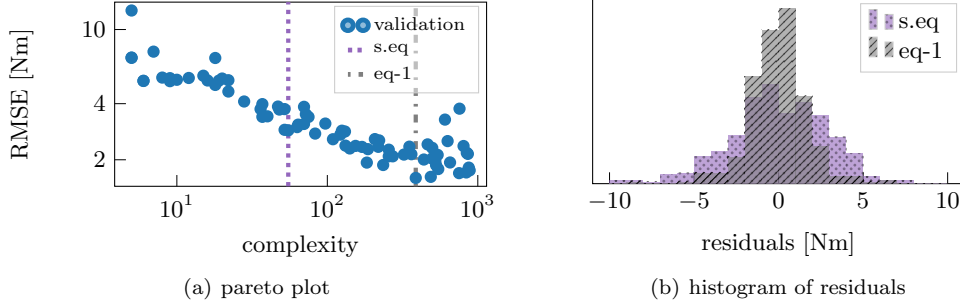


Figure 5: Equation learning with iEQL_{motor} on a real world dataset for torque of a combustion engine. Here, we show the run with median performance with the $V^{\text{int}}\text{-S}$ criteria. Panel (a) shows the pareto plot of the iEQL and (b) shows the histogram of residuals of the equation (s.eq) selected with the $V^{\text{int}}\text{-S}$ criteria and a more complex equation (eq-1).

Weights are indicated with w and bias with b . All selected equations can be simplified to the same equation $y = 0.4I_D^2 - 1.12I_D + 0.41I_Q^2 + 1.13I_Q - 0.31$. Numbers were rounded to three figures and input and output dimensions were anonymized. In addition, we emphasize that the algorithm learned that only two of the input variables, namely $[I_D, I_Q]$, are relevant to the output value, while the others have negligible influence.

4.4 Torque Model of an Internal Combustion Engine

A second task from the industrial domain is the modeling of the torque of a combustion engine in dependence of the control parameters. Ongoing improvements in power train technologies require more and more precise models for control strategies. This is commonly correlated with a complex structure of the models as well as the large number of calibration parameters. For utilization of those models in embedded systems it is essential to have fast development cycles, i.e. an automated adaptation to a new system, and low production costs. The unit costs grow with the computational needs on an embedded controller, thus computationally efficient at evaluation time is important. In practice, this leads often to a trade-off between accuracy of the model and its complexity.

In this dataset the engine torque is measured depending on exhaust camshaft ϕ_{ex} , intake camshaft ϕ_{in} , relative load r_l , ignition angle ϕ_{ign} and engine speed n_{eng} . The data was measured at stationary operation points. It contains 1775 data points measured at variations of the quantities listed in table 7 within their range of operation. The dataset is split into 80% training and 20% testing data and 10% of the train data set is used for validation.

Instance selection can be done with the V^{int} -S criteria or solely based on validation performance as long as the equation is computationally efficient at evaluation time. We present both solutions in table 6 alongside with the number of active parameters. The GP is supposed to perform best on this dataset, but the EQL-networks, selected with V^{int} , perform similar or even better. With about 170-470 parameters they are fast to compute and small enough to fit on embedded systems. The EQL $^+$ finds the best test RMSE results. This might indicate that for this dataset it is sufficient to deal with $\{\sin, \cos, *, \text{identity}\}$ units. Despite its larger expressive power, iEQL can compete with the EQL $^+$ architecture. GA is not able to learn equations that compete on the performance level, but it can identify simple equations with about 33 parameters. Yet, iEQL_{motor} also finds equations of similar complexity, but with a twice as good median test RMSE. Table 6 shows a noticeable relation between the performance of the models and their complexity for iEQL, iEQL_{motor} and EQL $^+$. The more complex the model the better its test RMSE. This effect occurs also in figure 5(a), which shows the pareto plot for the iEQL_{motor} experiment (median performance and V^{int} -S criteria). The histograms of residuals of the selected equation alongside with the best performing equation show no significant distribution shifts, see figure 5(b).

We analyze the equations of median performance and the equations with the smallest number of parameters selected with the V^{int} -S criteria for iEQL and iEQL_{motor} in appendix A.5. Their test RMSE is not as good as a GP, but their structure is interpretable. The motor specific complexity factors lead to equations of mainly polynomial structure with higher degree than without motor specific complexity factors. The latter combine polynomials with nonlinear units like \cos , \exp , \log or division units. Using more nonlinear units reduces the degree of the used polynomials. This is in agreement with the analysis of relative frequencies of atomic units shown in figure 4(a), which clearly shows that the use of motor specific complexity factors leads to a reduction of the use of $\{\log, \cos, \exp\}$ and division units and an increase of x^2 and multiplication units.

5 Conclusion

We introduced the informed equation learner iEQL. It aims to learn compact and interpretable models in form of concise mathematical equations from data. Our method differs from previous work in two key aspects: First, it is able to handle functional units with singularities in all hidden layers. Secondly, it can incorporate expert knowledge about the underlying system. To do so, prior knowledge is encoded in a complexity cost for individual atomic units. We evaluated our method by finding compact functional expressions for four different use cases: The iEQL performs well on established reference datasets. Customized priors can be applied to prefer certain functional terms in an ambiguous dataset supporting several possible explanations. Finally, we evaluated the algorithm on two real industrial problems. In both settings, the underlying relations of the system were unknown a priori, and the iEQL was able to extract simple, explainable models describing the respective output variable. Depending on the needs it also provides a high-performance solution with low computational cost.

Funding: Philipp Hennig and Georg Martius are members of the Machine Learning Cluster of Excellence, funded by the Deutsche Forschungsgemeinschaft (DFG, German Research Foundation) under Germany’s Excellence Strategy – EXC number 2064/1 – Project number 390727645. We acknowledge the support from the German Federal Ministry of Education and Research (BMBF) through the Tübingen AI Center (FKZ: 01IS18039B).

Authors’ contributions: All authors contributed to the conception and design of the study. Code preparation, data collection and analysis were performed by MW and supervised by GM and PH. AJ has supported the work as domain expert. The manuscript was drafted by MW and edited and reviewed by all authors.

References

- H. Akaike. Information theory and an extension of the maximum likelihood principle. In *Selected papers of hirotugu akaike*, pages 199–213. Springer, 1998.
- L. E. Ballentine. The Statistical Interpretation of Quantum Mechanics. *Reviews of Modern Physics*, 42(4):358–381, Oct. 1970.
- J. S. Buchner, S. Boblest, P. Engel, A. Junginger, and H. Ulmer. An artificial-intelligence-based method to automatically create interpretable models from data targeting embedded control applications. *IFAC*, 2020. 21th IFAC World Congress.
- M. Cranmer. Pysr: Fast & parallelized symbolic regression in python/julia, Sept. 2020. URL <http://doi.org/10.5281/zenodo.4041459>.
- R. Dubčáková. Eureqa: software review. *Genetic Programming and Evolvable Machines*, 12(2):173–178, Jun 2011. ISSN 1573-7632.
- R. P. Feynman, R. B. Leighton, and M. Sands. The feynman lectures on physics; vol. i. *American Journal of Physics*, 33(9):750–752, 1965.
- C. E. García, D. M. Prett, and M. Morari. Model predictive control: Theory and practice—a survey. *Automatica*, 25(3):335 – 348, 1989. ISSN 0005-1098.
- K. He, X. Zhang, S. Ren, and J. Sun. Identity mappings in deep residual networks. In *European Conference on Computer Vision (ECCV 2016)*, pages 630–645. Springer International Publishing, 2016.
- S. Hoffmann, M. Schrott, T. Huber, and T. Kruse. Modellbasierte Methoden zur Applikation moderner Verbrennungsmotoren. *MTZ*, 76(4):46–51, 2015.
- G. Huang, Z. Liu, L. van der Maaten, and K. Q. Weinberger. Densely connected convolutional networks. *2017 IEEE Conference on Computer Vision and Pattern Recognition (CVPR)*, pages 2261–2269, 2016.
- Y. Jin, W. Fu, J. Kang, J. Guo, and J. Guo. Bayesian symbolic regression. *arXiv preprint arXiv:1910.08892*, 2019.
- S. Kim, P. Y. Lu, S. Mukherjee, M. Gilbert, L. Jing, V. Čeperić, and M. Soljačić. Integration of neural network-based symbolic regression in deep learning for scientific discovery. *IEEE Transactions on Neural Networks and Learning Systems*, 2020.
- D. P. Kingma and J. Ba. Adam: A method for stochastic optimization. international conference on learning representations (2015), 2015.

- M. J. Kusner, B. Paige, and J. M. Hernández-Lobato. Grammar variational autoencoder. In *Proceedings of the 34th International Conference on Machine Learning-Volume 70*, pages 1945–1954. JMLR. org, 2017.
- G. Lample and F. Charton. Deep learning for symbolic mathematics. In *International Conference on Learning Representations*, 2020.
- W. B. Langdon, R. Poli, N. F. McPhee, and J. R. Koza. Genetic programming: An introduction and tutorial, with a survey of techniques and applications. In *Computational intelligence: A compendium*, pages 927–1028. Springer, 2008.
- L. Li, M. Fan, R. Singh, and P. Riley. Neural-guided symbolic regression with semantic prior. *arXiv preprint arXiv:1901.07714*, 2019.
- S.-C. Lin, G. Martius, and M. Oettel. Analytical classical density functionals from an equation learning network. *The Journal of Chemical Physics*, 152(2):021102, 2020.
- Z. Long, Y. Lu, and B. Dong. PDE-Net 2.0: Learning PDEs from data with a numeric-symbolic hybrid deep network. *Journal of Comp. Physics*, 399:108925, 2019. ISSN 0021-9991.
- C. Louizos, M. Welling, and D. P. Kingma. Learning sparse neural networks through l_0 regularization. In *International Conference on Learning Representations*, 2018.
- D. J. MacKay. Bayesian interpolation. *Neural computation*, 4(3):415–447, 1992.
- C. J. Maddison, A. Mnih, and Y. W. Teh. The concrete distribution: A continuous relaxation of discrete random variables, 2016.
- G. Martius and C. H. Lampert. Extrapolation and learning equations, 2016. arXiv <https://arxiv.org/abs/1610.02995>.
- R. K. McRee. Symbolic regression using nearest neighbor indexing. In *Proceedings of the 12th Annual Conference Companion on Genetic and Evolutionary Computation, GECCO '10*, pages 1983–1990, New York, NY, USA, 2010. ACM. ISBN 978-1-4503-0073-5.
- T. J. Mitchell and J. J. Beauchamp. Bayesian variable selection in linear regression. *Journal of the American Statistical Association*, 83(404):1023–1032, 1988.
- B. K. Petersen. Deep symbolic regression: Recovering mathematical expressions from data via policy gradients. *arXiv preprint arXiv:1912.04871*, 2019.
- S. S. Sahoo, C. H. Lampert, and G. Martius. Learning equations for extrapolation and control. In *International Conference on Machine Learning, ICML 2018*, volume 80, pages 4442–4450. PMLR, 2018.
- M. Schmidt and H. Lipson. Distilling free-form natural laws from experimental data. *Science*, 324(5923):81–85, 2009. ISSN 0036-8075.
- G. Schwarz et al. Estimating the dimension of a model. *The annals of statistics*, 6(2):461–464, 1978.
- D. P. Searson, D. E. Leahy, and M. J. Willis. GPTIPS: an open source genetic programming toolbox for multigene symbolic regression. In *International Multi-conference of Engineers and Computer scientists*, volume 1, pages 77–80. IMECS Hong Kong, 2010.
- R. Tibshirani. Regression shrinkage and selection via the lasso. *Journal of the Royal Statistical Society: Series B (Methodological)*, 58(1):267–288, 1996.

- L. Trujillo, L. Muñoz, E. Galván-López, and S. Silva. neat genetic programming: Controlling bloat naturally. *Information Sciences*, 333:21–43, 2016. ISSN 0020-0255.
- S.-M. Udrescu and M. Tegmark. Ai feynman: A physics-inspired method for symbolic regression. *Science Advances*, 6(16):eaay2631, 2020.
- R. J. Williams. Simple statistical gradient-following algorithms for connectionist reinforcement learning. *Machine learning*, 8(3-4):229–256, 1992.
- W. Zaremba, K. Kurach, and R. Fergus. Learning to discover efficient mathematical identities. In *Advances in Neural Information Processing Systems*, page 1278, 2014.

A Appendix

A.1 iEQL Training

All experiments are performed using an iEQL with four hidden layers. Each hidden layer has $\{\cos, \exp, \log, \sqrt{\cdot}, x^2, *, /\}$ as atomic units, and each atomic unit is applied four times in each layer. We prohibit the following combinations $\cos(\cos)$, $\cos(\exp)$, $\exp(\exp)$, $\log(\log)$. The iEQL has thus 6405 learnable weights. Training is executed in two phases. In phase 1 we train for $T_1 = 2000$ epochs without regularization. This phase overcomes bad initialization and assures that the model is close to a minimum when pruning starts. In phase 2 we train for $T_2 = 10000$ epochs with regularization strength λ . Just for the combustion engine dataset, which has about 5 to 6 times fewer data points, we increased the number of epochs by a factor of 8. We skipped train phase 1 for the ambiguous dataset since the iEQL is already sufficiently close to a minimum. After each epoch, an intrinsic penalty epoch is calculated with 100 randomly sampled data points from the test domain (without labels). The maximum desired output value is set to $B = 10$ with $\eta = 1$. We use the ADAM optimizer [Kingma and Ba, 2015] with learning rate 0.001, moving average $\beta_1 = 0.4$ and $\epsilon = 10^{-8}$ for numerical stability. The initial dropout rate of the Bernoulli gates is set to 0.5 and the domain/bound penalty strength is set to $\delta = 1$. Further information on dropout rate is given in appendix 3.4. Since the optimal regularization scale parameter λ is not known in advance, we train several models with different regularization strengths $\lambda = 10^k$ where k is in the range from -5.0 to 0.0 with 78 equally spaced steps. This results in 78 equations with different complexities and root mean squared errors (RMSE).

Baselines:

We calculate the mean predictor (MP) on the train set and a multi-layer perceptron (MLP) with tanh activation functions and five hidden layers with 50 neurons each. It is trained with batch size 100 for 5000 epochs and the ADAM optimizer with a learning rate of 0.001 and $\beta_1 = 0.9$. A grid search on the learning rate revealed that it is pretty robust in the range $[0.001, 0.0001]$. We select the best validation model to avoid overfitting.

We compare to EQL⁺, a state-of-the-art method from Sahoo et al. [2018] with atomic unit types $\{\sin, \cos, *, \text{identity}\}$ and division in the final layer. It is sufficient to use the hyperparameters proposed in Sahoo et al. [2018] since the datasets on which we compare have similar properties to the ones in Sahoo et al. [2018]. So we applied, ADAM optimizer with learning rate 0.001 and $\epsilon = 10^{-4}$, mini-batch size 20, domain penalty $\eta = 10$ with $B = 10$, and 10 atomic units per type in each layer. The number of total epochs is given by $T = (L - 1) \cdot 10,000$, where L is the number of hidden layers. Just for the combustion engine dataset, which has about 5 to 6 times fewer data points, we had to increase the number of total epochs to $T = (L - 1) \cdot 80,000$. We perform model selection amongst the following parameters: regularization strengths $\lambda = 10^k$ where k is in the range from -6.0 to -3.5 with 26 equally spaced steps and $L \in \{2, 3, 4\}$. This results in 78 equations with different complexities and root mean squared errors (RMSE).

Another baseline is (PySR, Cranmer [2020]) a genetic algorithm for symbolic regression with hyperparameters shown in table 8 for two different configurations (GA1, GA2). Both settings turned out to perform well on different datasets. We had to restrict the size of the datasets to 1000 data points in order to avoid exploding memory size. We do not compare to EUREQA, the current state-of-the-art tool for symbolic regression [Dubčáková, 2011], since it has become proprietary and was merged into an online service.

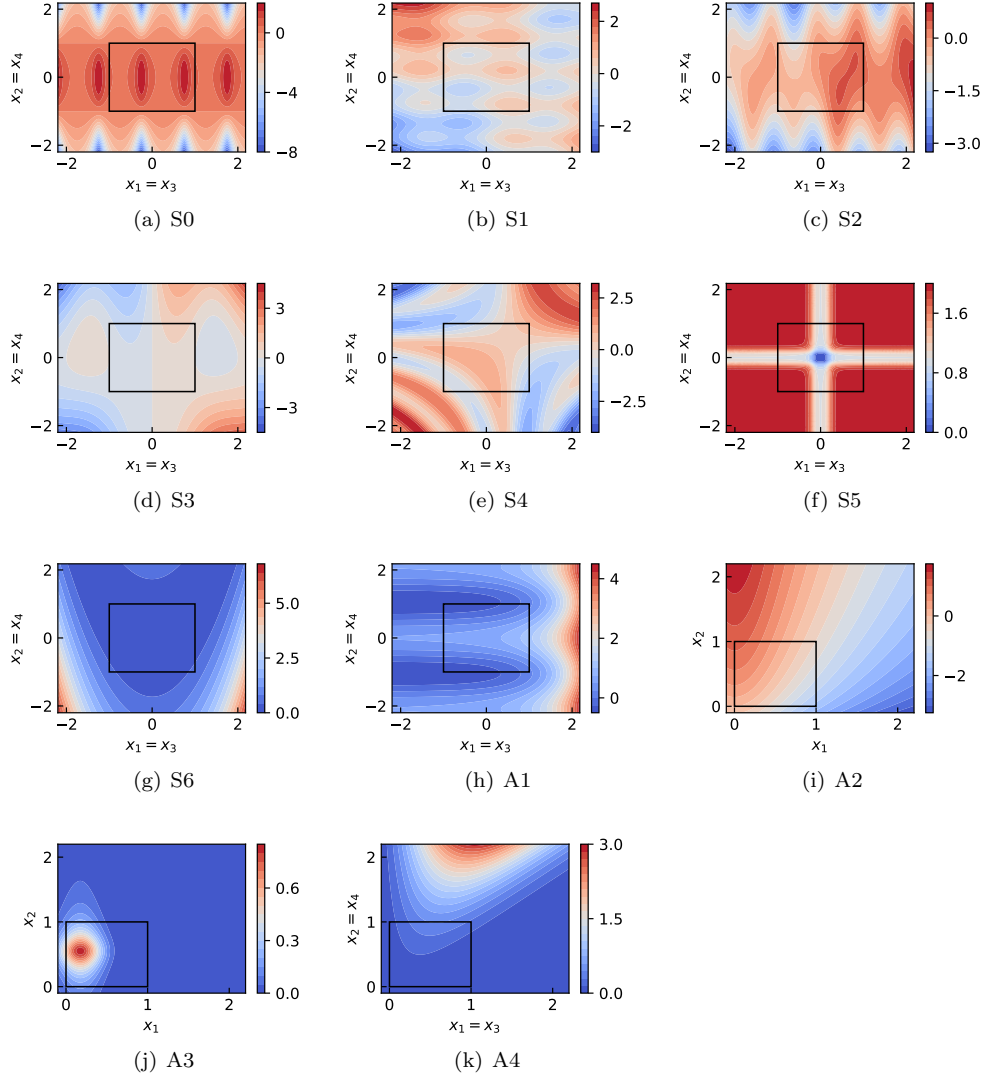


Figure 6: Two dimensional slices through the input space of simulated equations S0–S6 and A1–A4 from table 2. The black rectangle indicates the train domain.

Table 8: Tuned hyperparameters for the genetic algorithm [Cranmer, 2020].

	GA1	GA2
niterations	40	10
npop	1000	1000
populations	60	30
binary operators	$\{\pm, *, /\}$	$\{\pm, *, /\}$
unary operators	$\{\cos, \exp, \log\}$	$\{\cos, x^2, \exp, \log\}$
maxsize	40	40
parsimony	0	0
warmupMaxsizeBy	0.5	0
useFrequency	False	True
annealing	False	False
optimizer algorithm	BFGS	BFGS
optimizer iterations	100	100
procs	30	30

For the real world datasets a Gaussian Process (GP) is calculated with ASCMO [Hoffmann et al., 2015], a standard tool from the engineering domain.

A.2 Power Loss of an Electric Machine

Here, we present details on the preparation of training and test dataset. First, 20% of the whole dataset is used for testing and excluded from training. Then, the train domain is restricted to 80% of its range of operation ($[a, b] \rightarrow [0.8a, 0.8b]$ for each dimension). Rotor temperature T_{rot} is not restricted, since it consists just of three different operation points. Further, 10% of the train dataset is used for validation. Restricting the train domain assures that the test dataset contains samples from an extrapolation domain as well as samples from the train domain.

A.3 Sparsity Inducing Method

In this section we outline the L_0 regularization by Louizos et al. [2018] in more detail, which is used in our sparsity inducing method. For simplicity the complexity factors c_u are neglected, since it is straightforward to integrate them. The objective function we want to optimize is given by

$$\mathcal{L} = \frac{1}{N} \sum_{i=1}^N \|\mathbf{y}_i - \text{iEQL}(\mathbf{x}_i, \mathbf{W})\|_2^2 + \lambda \|\mathbf{W}\|_0. \quad (17)$$

The L_0 -norm counts the number of non-zero weights, which total number is denoted by $|\mathbf{W}|$. Specific choices of the scale parameter λ refer to well-known model selection criteria as the Bayesian Information Criterion (BIC, Schwarz et al. [1978]) and the Akaike Information Criterion (AIC, Akaike [1998]). Each weight of the iEQL is multiplied by a non-negative stochastic Bernoulli distributed gate

$$w_i = \tilde{w}_i \cdot g_j \quad q(g_j \mid \pi_j) = \text{Ber}(\pi_j). \quad (18)$$

The dropout rate of each weight is thus given by $1 - \pi_j$. The expectation of a weight being relevant is given by π_j . Those gates learn collectively which weights are relevant. The expected objective is then

$$\mathcal{L} = \mathbb{E}_{q(\mathbf{g}|\boldsymbol{\pi})} \left[\frac{1}{N} \sum_{i=1}^N \|\mathbf{y}_i - \text{iEQL}(\mathbf{x}_i, \mathbf{W})\|_2^2 \right] + \lambda \sum_{j \leq |\mathbf{W}|} \pi_j. \quad (19)$$

This objective can be described as a special case of a variational bound over weights with spike and slab [Mitchell and Beauchamp, 1988] priors and approximate posteriors. We refer the interested reader to appendix A of Louizos et al. [2018] for further details.

A.3.1 Reparameterization Trick

In order to apply gradient based optimization the objective is smoothed. Therefore, the gates z are hard-sigmoid rectifications $b(\cdot)$ of a continuous random variable s with variables ϕ

$$s \sim q(s | \phi), \quad z = b(s), \quad \text{with: } b(\cdot) = \min(1, \max(0, \cdot)). \quad (20)$$

The expected loss is then

$$\mathcal{L} = \mathbb{E}_{q(s|\phi)} \left[\frac{1}{N} \sum_{i=1}^N \|\mathbf{y}_i - \text{iEQL}(\mathbf{x}_i; \mathbf{W} \odot b(s))\|_2^2 \right] + \lambda \sum_{j \leq |W|} (1 - Q(s_j \leq 0 | \phi_j)) \quad (21)$$

with the cumulative distribution (CDF) $Q(\cdot)$ of s . This penalizes the probability of a gate being non-zero. By choosing a suitable continuous distribution $q(s)$ we can apply the reparameterization trick with parameter free noise distribution ϵ and a deterministic and differentiable transformation $f(\cdot)$

$$\mathcal{L} = \mathbb{E}_{p(\epsilon)} \left[\frac{1}{N} \sum_{i=1}^N \|\mathbf{y}_i - \text{iEQL}(\mathbf{x}_i; \mathbf{W} \odot b(f(\phi, \epsilon)))\|_2^2 \right] + \lambda \sum_{j \leq |W|} (1 - Q(s_j \leq 0 | \phi_j)) \quad (22)$$

The final reparameterization is given by the hard concrete distribution, which is outlined in the following.

A.3.2 Hard Concrete Distribution

s is a binary concrete random variable (Maddison et al. [2016], He et al. [2016]) by choice, distributed over $(0, 1)$ with probability density $q(s | \phi)$ and cumulative density $Q_\beta(s | \phi)$. The distribution has two parameters. Its location is denoted by $\log \alpha$ and the degree of approximation is controlled by β . A sampling method for the stretched version for the interval (γ, ζ) is given by

$$u \sim U(0, 1) \quad (23)$$

$$s = \text{Sigmoid}((\log u - \log(1 - u) + \log \alpha) / \beta) \quad (24)$$

$$\bar{s} = s(\zeta - \gamma) + \gamma \quad (25)$$

$$z = b(\bar{s}) \quad (26)$$

with more details

$$q_s(s | \phi) = \frac{\beta \alpha s^{-\beta-1} (1-s)^{-\beta-1}}{(\alpha s^{-\beta} + (1-s)^{-\beta/2})^2} \quad (27)$$

$$Q_s(s | \phi) = \text{Sigmoid}((\log s - \log(1-s))\beta - \log \alpha) \quad (28)$$

$$q_{\bar{s}}(\bar{s} | \phi) = \frac{1}{|\zeta - \gamma|} q_s\left(\frac{\bar{s} - \gamma}{\zeta - \gamma} | \phi\right) \quad (29)$$

$$Q_{\bar{s}}(\bar{s} | \phi) = Q_s\left(\frac{\bar{s} - \gamma}{\zeta - \gamma} | \phi\right) \quad (30)$$

and finally the hard sigmoid z we obtain the distribution

$$q(z | \phi) = Q_{\bar{s}}(0 | \phi)\delta(z) + (1 - Q_{\bar{s}}(1 | \phi))\delta(z - 1) + (Q_{\bar{s}}(1 | \phi) - Q_{\bar{s}}(0 | \phi))q_{\bar{s}}(z | \bar{s} \in (0, 1), \phi) \quad (31)$$

Thus the complexity loss is given by

$$\mathcal{L}_C = \text{Sigmoid} \left((\log \alpha - \beta \log \frac{-\gamma}{\zeta}) \right) \quad (32)$$

and for final estimation of the parameters under a hard concrete gate:

$$\hat{z} = \min(1, \max(0, \text{Sigmoid}(\log \alpha)(\zeta - \gamma) + \gamma)) \quad (33)$$

In our implementation we use the same hyperparameters as Louizos et al. [2018]

$$\zeta = 1.1, \quad \gamma = -0.1, \quad \beta = 2/3. \quad (34)$$

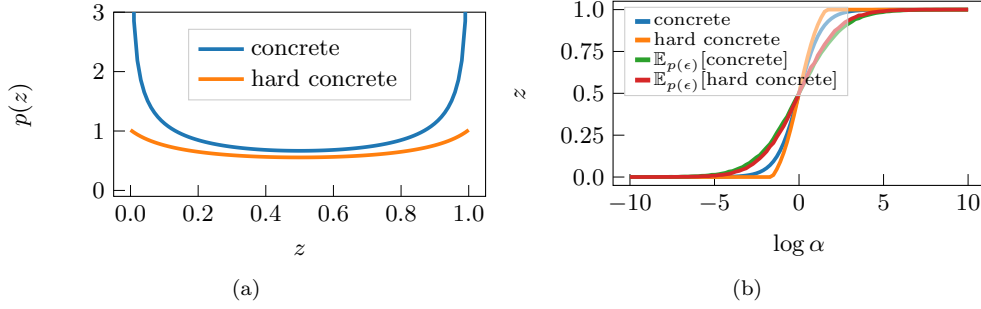


Figure 7: The probability density function for the concrete gate (equation 28) and hard concrete gate (equation 30) are shown in (a) and their expectation (equation 24 and equation 26 respectively) for 10,000 samples are shown in (b). We added the concrete and hard concrete without noise as well. All plots are produced with the hyperparameters mentioned in equation 34.

A.4 Model Selection Criteria

Both criteria $V^{\text{int}\&\text{ex}}$ and $V^{\text{int-S}}$ perform similarly good on equations (S0–S6), but the $V^{\text{int}\&\text{ex}}$ methods performs better on the more sophisticated equations (A1–A4). However, it requires additional extrapolation data points, which might not be available in real world datasets. Therefore, we apply the $V^{\text{int-S}}$ method on the two real world datasets.

To illustrate the importance of the equation selection process we evaluate the selected equation alongside with a simpler and a more complex solution on the S0 dataset, see figure 8. If the selected equation is too complex its validation loss is at noise level, but it is not able to extrapolate, as seen e.g. in the left panel of figure 8. If the selected equation is too simple validation and extrapolation loss are not at noise level.

A.5 Different Combustion engine Equations

We present the equations of median performance and the equations with the smallest number of parameters selected with the $V^{\text{int-S}}$ criteria for iEQL and iEQL_{motor}. An

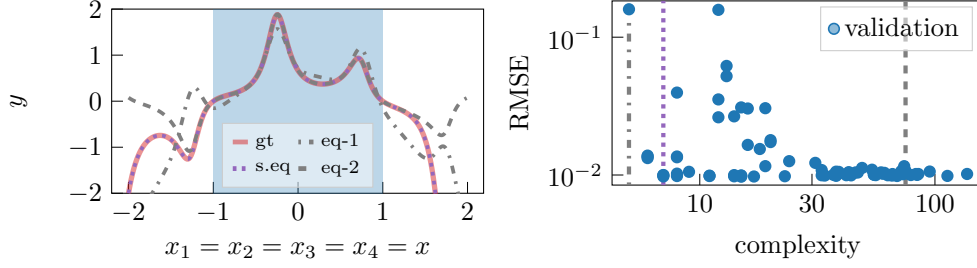


Figure 8: The panel in the left column displays a slice through the input space of equation S0. The blue shading indicates the train domain. The selected equation (dotted line) was determined with the $V^{\text{int}\&\text{ex}}$ selection criteria. Additionally, a too simple (dashdotted line) and too complex equation (dashed line) are plotted for comparison. The right column shows the corresponding pareto plot. Each point corresponds to an independent run of the iEQL with a different complexity regularization. The three equations shown on the left are marked with corresponding vertical lines.

Table 9: Overview of analysed iEQL expressions on the combustion engine dataset. The RMSE on the test dataset with the number of active parameters is shown.

iEQL	RMSE [Nm]	#parameters	equation
motor simple	6.16	15	35
motor median	3.17	32	36
plain simple	3.04	42	37
plain median	2.48	79	38

overview of all four analyzed equations on the combustion engine dataset is shown in table 9. Numbers were rounded to three figures and input and output dimensions were anonymized. The motor specific complexity factors lead to equations of mainly polynomial structure with higher degree than without motor specific complexity factors. The latter combine polynomials with simple nonlinear units like cos, exp, log or division units. Using more nonlinear units reduces the degree of the used polynomials.

iEQL_{motor} simple:

- compact notation of a polynomial of degree 8

$$y = 2.48x_2 + 0.66(0.3x_2 + 0.79)(-0.8x_1 + 1.86x_3 - 0.08) - 0.52\left(-2.13x_3 + 0.57(0.05 - 1.19x_3)^2 - 0.62(-0.89x_1 + 0.85(0.46x_1 - 0.32)(1.28x_3 + 0.34x_5 + 0.71) + 0.42)^2 + 0.56\right)^2 + 0.94 \quad (35)$$

iEQL_{motor} median:

- compact notation of a polynomial of degree 7
- cos units in final layer with previous polynomial terms as arguments.

$$y = -0.3x_1 + 2.32x_2 + 0.27x_3 + 0.6c_2 + 0.3c_3 + 0.35 \cos(1.12x_3 + 1.42c_2 + 0.59c_3 - 0.23) + 0.51 \quad (36)$$

substitutions:

$$\begin{aligned} c_1 &= (0.05 - 0.69x_1)(1.0x_1 + 0.64) \\ c_2 &= (-0.95x_2 - 0.69)\left(-1.06x_3 + 0.96(-0.21x_1 + 0.66x_3 - 1.01)^2 - 1.2\right) \\ c_3 &= \left(-0.74x_3 - 0.76\left(0.6x_1 + 0.73c_1 + 0.47(0.76x_2 + 0.19x_4 - 0.19x_5 - 0.6)^2 - 0.9\right)^2 + 1.36\right) \\ &\quad (2.0x_3 + 0.88(-0.73x_1 - 1.17c_1 + 0.26)(0.6x_4 - 0.72x_5 - 0.46) - 0.31) \end{aligned}$$

iEQL simple:

- polynomial of degree 4 with simple cos and exp units
- cos units with previous polynomial terms as arguments.

$$\begin{aligned}
y = & 1.49x_2 + 0.53(0.94x_2 + 0.8)(1.89x_3 - 0.29\cos(4.79x_3 + 2.83) + 0.46) \\
& + 0.81e^{-0.27x_1+0.18x_2} + 0.94e^{-0.32x_1+0.25x_2+0.55x_3} - 0.05c_1 \\
& + 0.22\cos(1.45x_3 - 1.02c_2 + 0.07) - 0.29\cos(0.66x_2 - 1.13c_2 - 0.74c_3 + 2.73) \\
& - 0.23\cos(-1.21x_1 + 1.99x_3 - 2.26(-0.94x_2 - 0.52)(0.97x_3 + 0.02) - 0.97c_3 + 3.71) - 1.71
\end{aligned} \tag{37}$$

substitutions:

$$\begin{aligned}
c_1 &= \cos(4.0x_1 + 2.38) \\
c_2 &= \left(-0.49x_1 + 1.1x_3 + 0.76(1.02x_1 - 0.02)^2 - 0.85\right)^2 \\
c_3 &= (-0.41x_2 - 0.53x_3 - 0.29x_4 + 0.34x_5 + 0.59(0.07 - 0.97x_1)(0.28 - 1.02x_2) + 0.23c_1 + 0.6)^2
\end{aligned}$$

iEQL median:

- polynomial of degree 4 with simple cos, log and division units
- division units occur also in intermediate layers
- cos units with previous polynomial terms as arguments

$$\begin{aligned}
y = & 2.0x_2 + 0.6x_3 + 0.06x_4 - 0.05x_5 - 0.49(0.83x_2 + 0.58)(-0.81x_3 - 0.42) + \frac{0.39(0.99x_2 + 0.79)}{6.75(1.77c_1 - 0.75)^2 + 1.96} \\
& - 0.24(-0.77x_2 - 0.36c_1 - 0.42)\left(1.11x_3 + 0.32c_2 - 0.89(-1.1x_3 + 0.73c_1 + 0.41)^2\right. \\
& \quad \left. - 0.47\cos(5.98x_3 + 3.27) + 0.09\right) \\
& - 0.29\left(-0.78x_2 + 0.35(1.77c_1 - 0.75)^2 + 0.35\cos(1.72x_2 - 2.6) - 0.67\right)^2 \\
& - 0.28c_3 + 0.18\log(1.08 - 0.88x_1) - 0.2\cos(-1.21x_2 + 1.28c_3 + 4.61) \\
& - 0.15\cos(1.95x_2 + 1.58x_3 + 1.0c_4 + 3.51) \\
& + 0.18\cos(0.77x_1 - 1.71x_2 - 0.76c_4 + 0.71c_3 + 1.51) + 0.74 - \frac{0.39(0.85x_1 - 0.58)}{3.29 - 2.85x_2}
\end{aligned} \tag{38}$$

substitutions:

$$\begin{aligned}
c_1 &= \cos(2.07x_1 + 0.21x_2 - 0.02) \\
c_2 &= (0.33x_1 + 1.09c_1 + 0.51)(-0.74x_4 + 0.61x_5 + 1.02c_1 - 0.62) \\
c_3 &= \left(0.29x_1 - 1.65x_3 - 0.09x_4 + 0.09x_5 - 0.27(-0.69x_1 - 0.14)^2 + 0.35(0.68x_1 - 1.27x_3 + 0.3)^2 + 0.4\right)^2 \\
c_4 &= \left(-0.43x_4 + 0.36x_5 + 0.8 + \frac{0.86(-1.22x_2 - 0.94x_3 - 0.66)}{2.11x_1 + 2.35}\right) \\
& \quad (0.6x_2 + 1.28x_3 + 0.89x_4 - 1.18x_5 + 0.77c_2 - 0.05)
\end{aligned}$$